PID Techniques: Alternatives to RICH Methods

J. Va'vra

SLAC National Accelerator Laboratory, CA, USA

Abstract – **In this review article we discuss the recent progress in PID techniques other than the RICH methods. In particular we mention the recent progress in the Transition Radiation Detector (TRD), dE/dx cluster counting, and Time Of Flight (TOF) techniques.**[1]

INTRODUCTION

Figure 1 shows the typical reach of various PID techniques used in present experiments. The transition radiation detector (TRD) technique is typically used to identify electrons in hadron colliders. It is a mature and well understood method, and has been proven to work well. It needs a lot of longitudinal or radial detector space, typically ~20cm for every π/e rejection factor of 10. The TOF technique is useful in e^+e^- colliders to identify hadrons below a few GeV. The dE/dx technique has been described many times before, and therefore here we want to concentrate only on cluster counting, which may provide better performance. Although none of these methods compete with the performance of the RICH technique across such a broad energy range, they are generally less complex, may cover a lower momentum range, and, are in principle cheaper.
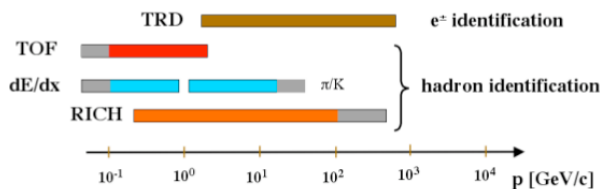
Fig. 1 Typical reach of PID techniques described in this paper.

The radiation environment in some of the new experiments is severe. Table 1 shows typical conditions at SuperB, Belle II, LHC and ALICE heavy ion collisions. For example, the pp-diffractive scattering at LHC will have to cope with proton rates up to 10-15MHz/cm^2 and total accumulated neutron doses up to ~10^{12}/cm^2. Even high luminosity e^+e^- colliders, such as SuperB or Belle II, will have to deal with huge neutron doses of up to 10^{12}/cm^2 after 10 years of running. All this means that designers of these experiments have very severe challenges, which will undoubtedly lead to problems and required upgrades.

Table 1: Background challenges of future experiments.

TRANSITION RADIATION DETECTORS (TRD)

A particle passing through a dielectric boundary emits photons with some probability. The radiated power is proportional to the ~γ factor of the particle, but the number of emitted photons is small and proportional to $\alpha \sim 1/137$, and the opening angle is also small and proportional to $1/\gamma$. The emitted photon energy is typically between 2 and 15 keV. The TRD concept is used to identify electrons, as their γ-factor can be sufficiently high. To increase the probability of emission, one wants to use many dielectric boundaries within the detector, for example, using polypropylene foam [1]. This was used as a radiator of transition radiation in the ATLAS central tracker[2] (see Fig.2a). Figure 2b shows a typical pulse height spectrum from the ATLAS TRD detector in the test beam, and Fig.2c shows the first LHC results [1].

A TRD detector needs substantial detector space. Typically, an order of magnitude in rejection power against pions is gained each time the TRD detector length is increased by ~20cm. Table 2 lists several experiments, which contain TRDs, with the typical π rejection factors achieved.

[1] Invited talk at RICH 2010, May 5, Cassis, France

[2] ATLAS central tracker [1] uses straw tubes (425k channels), filled with 70%Xe + 27% CO$_2$ + 3%O$_2$ gas, and operating at a gain of 2x10^4.

(a)

(b)

(c)
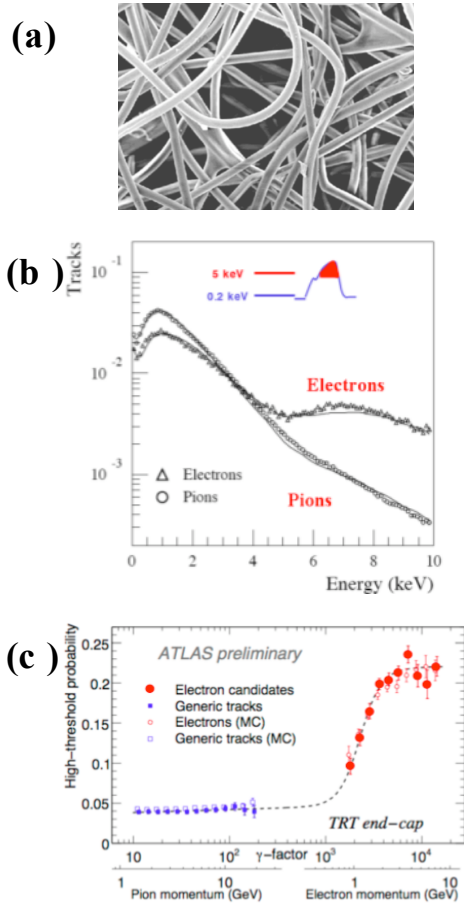
Fig. 2 (a) Photomicrograph of a radiator for transition radiation: polypropylene foam with many dielectric boundaries, as used in the ATLAS TRD central straw tracker. (b) Test beam results with ATLAS test chamber. (c) Preliminary results from ATLAS detector operating at LHC.

Table 2: Experiments employing TRD detectors [1].

Experiment	Gas	L (cm)	No of channels	$\pi_{rejection}$
HELLIOS (NA34)	$Xe-C_4H_{10}$	70	1744	2000
H1	$Xe-He-C_2H_6$	60	1728	10
NA31	$Xe-He-CH_4$	96	384	70
ZEUS	$Xe-He-CH_4$	40	2112	100
D0	$Xe-CH_4$	33	1536	50
NOMAD	$Xe-CO_2$	150	1584	1000
kTeV	$Xe-CO_2$	144	~10k	250
PHENIX	$Xe-CH_4$	4	43k	300
PAMELA	$Xe-CO_2$	28	964	50
AMS	$Xe-CO_2$	55	5248	1000
ATLAS	$Xe-CF_4-CO_2$	51-108	425k	100
ALICE	$Xe-CO_2$	52	1.2 M	200

dE/dx CLUSTER COUNTING

The dE/dx particle separation in terms of number of sigmas is $N_\sigma = [dE/dx(m_1)-dE/dx(m_2)]/\sigma$, where dE/dx [keV/cm] is the average energy deposit in a given sample, m_1 and m_2 are masses of two particles and σ is an error of the measurement. A classical dE/dx method integrates the total charge in a given

drift cell track segment. Values of dE/dx and σ can be predicted easily semi-empirically, for example, as shown in [10]. For typical Ar-based or He-based gases, and a 1cm-long sample at 1 bar, one obtains the resolution of FWHM/(dE/dx) ~100%. This value can be improved significantly if one determines the energy deposit instead by the cluster counting.

Cluster counting has been studied extensively in the past [2-8], both theoretically and experimentally. To resolve individual ionization clusters, two methodologies have been studied: (a) either a time expansion chamber, where ions drift in a very low electric field, or, (b) employing low gas pressure. Neither method is very practical in the modern drift chambers considered at high luminosity colliders, such as SuperB. Instead, to resolve individual clusters, it is suggested [9] to use a He-based gas with no more than 5% of quencher, such as iC_4H_{10} gas. The He gas has 5.5±0.9 primary clusters/cm at 1 bar, and iC_4H_{10}-gas has 70±12 primary clusters/cm. Figure 3a shows that 95% He+5% iC_4H_{10}-gas at 1 bar has ~35 primary clusters per 2.6cm of drift cell [9]. One can see that there is a small tail due to delta rays, which will have to be dealt with by a truncated mean method. This is, however, nowhere near as large in magnitude as a typical Landau tail one observes in the classical dE/dx method, which integrates the charge from the entire track sample. Figure 3b shows the measured and simulated pulses from clusters in the same cell [9]. Clearly, a challenge of this method is to fine-tune the amount of iC_4H_{10} so that one has a large enough number of clusters but not too large to prevent reliable counting.

To illustrate the dE/dx performance improvement with the cluster counting, we take 95%He+5%iC_4H_{10} gas, with a 1 cm long drift sample. We obtain $N_{primary\_ions}$ ~15 and therefore we expect FWHM/(dE/dx) $\sim 2.35\sqrt{N_{primary\_ions}}/N_{primary\_ions} \sim 60\%$.

(a)   **(b)**
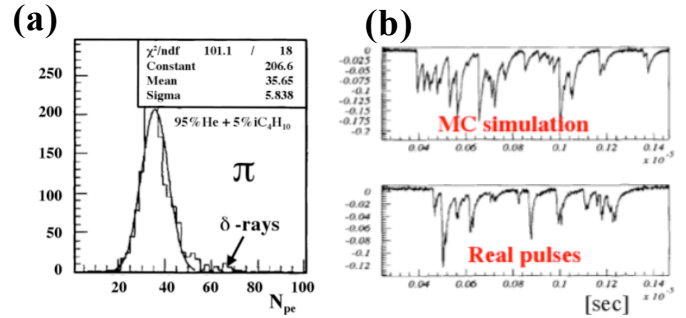
Fig. 3 (a) Number of primary clusters in a 2.6cm long drift cell with 95%He+5% iC_4H_{10} gas at 1 bar. (b) Measured and simulated numbers of primary clusters in the same gas [9].

Figure 4 shows my prediction of the proposed SuperB drift chamber performance with cluster counting and compares it to a classical dE/dx method. The calculation uses a dE/dx separation model as described in [10], and combines it with a resolution based on a scaled number of clusters for forward tracks going through a 1.2cm-long drift cell at 45°, and 95% He+5% iC_4H_{10}-gas, based on [9]. The graph also shows that the dE/dx "hole" near ~1 GeV/c could be "filled" with a TOF counter operating with ~ 100ps resolution.
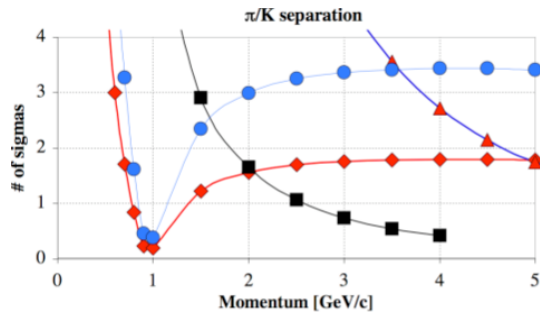
Fig. 4 Author's prediction of the pi/K separation obtained using the "cluster counting" method in a SuperB drift chamber for tracks in the forward region for a dip angle of 45° (circles), compared to the predicted classical dE/dx performance for a dip angle 90° (diamonds). The graph also shows the predicted performance of a forward PID with a TOF detector having σ ~100ps resolution (squares), which would be enough to "fill" the dE/dx hole near ~1 GeV/c. For comparison, we show also the predicted FDIRC RICH performance.

TIME-OF-FLIGHT (TOF)

The TOF particle separation in terms of number of sigmas is $N_\sigma = [(L_{path}c/2p^2)(m_1^2-m_2^2)]/\sigma$, where L_{path} is a path length, c is velocity of light, p is a particle momentum, m_1 and m_2 are masses of two particles, and σ is the error of the time measurement. The error σ is influenced by many factors such as the detector transit time spread (σ_{TTS}), electronics, photon radiator, bunch length, track length, chromatic effects, and many other detailed effects. The hardest parts to deal with, but which contribute significantly to the TOF performance, are the contribution from the detector (through σ_{TTS}) and the electronics, and that is why this paper will concentrate its effort in these two areas.

A. MRPC detectors

The concept was developed from the Resistive Plate Chambers (RPCs) [11-13], and perfected further, for example, by Williams and his collaborators at ALICE [14,15]. Other experiments used MRPC detectors (STAR[3] [16]), or are planning to use them (CBM[4] [17]). MRPC detectors are multi-gap glass RPC detectors, which can reach extremely good timing resolution. The gap size is only ~250µm to prevent a development of sparks. Because a large signal is developed only if an electron is produced very near the cathode, one needs many gaps to reach high enough efficiency. Figures 5a&b show the MRPC concept of the ALICE experiment [14,15,18]. The electrical contact is made only to the outer glass plates, the inner ones are electrically floating. Simple fishing nylon lines maintain precise gap dimensions. The MRPC detectors are easy to build even for large area coverage. Table 3 shows the operating parameters of the ALICE MRPC design.

Fig. 5 ALICE MRPC: (a) side view showing 10 gaps, (b) top view showing a nylon line used as a spacer between glass plates, and (c) This graph shows the power of combining the information from the TPC's dE/dx and the TOF MRPC. This particular graph is based on initial preliminary TOF resolution of ~130ps [18].

ALICE has reached a timing resolution of σ ~41ps in the test beam [15,18]. Various contributions to it were as follows: $\sigma_{NINO\ ASIC+cables}$ ~ 21ps, $\sigma_{Beam\ spot}$ ~14ps, σ_{MRPC} ~ 11ps, and σ_{TDC} ~30ps, which already indicates that the MRPC contribution is close to ~10ps. The initial resolution in ALICE at LHC is about 130ps at present. However, not all corrections were yet worked out. But even this resolution allows a very good PID performance when combined with the dE/dx method (see Fig.5c).

Table 3: Parameters of ALICE MRPC detectors

Parameter	Value
Total number of active gaps per MRPC & total in ALICE	10 / MRPC & 160,000 total in ALICE
Gap size (controlled by a fishing line)	250 µm
Glass size in one MRPC & total in ALICE	1200 x 72 mm² & 150 m² in ALICE
Pad geometry & number of pads/MRPC	25 x 36 mm² & 96 pads /MRPC
Gas	90% $C_2F_4H_2$ + 5% iC_4H_{10} + 5% CF_6
Signal rise time	~500 ps
Average total charge	~ 2pC / MRPC
Typical counting rate	~ 100 Hz/cm² (max rate: ~ 1kHz/cm²)
Total mass per MRPC with 10 gaps	~ 6% of r.l. / particle passage
Magnetic field in ALICE	16 kG
Pulse height correction	Leading & trailing edge timing (TOT)

---

[3] STAR 8-gap MRPC has reached a resolution of σ ~60ps.
[4] CBM experiment is looking into new MRPC geometries including a strip line readout.

In order to find the MRPC timing resolution limit, the ALICE group has performed a beam test with a new design [18] shown in Fig.6a. A number of improvements were implemented: (a) faster amplifier mounted directly on the MRPC, (b) read out both sides of the pad, and (c) increased number of gaps. The beam test result of ~16ps per single MRPC is shown in Fig.6b, where the MRPC contribution to the final resolution is σ_{MRPC} <10ps, and the limiting factor is believed to be the electronics[5].

(a)

(b)
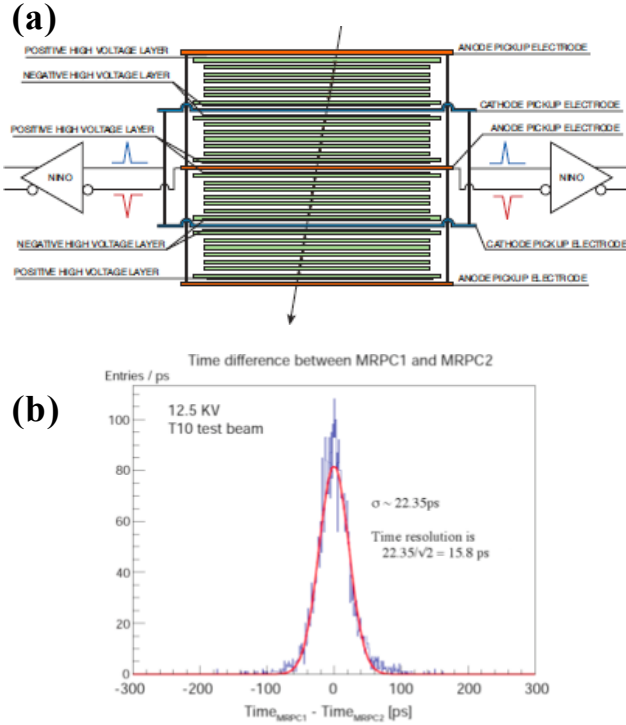
Fig. 6 (a) MRPC prototype with 24-gaps (160μm/gap), and 14% r.l./MRPC. Two identical MRPCs were used in the test beam. (b) Resolution obtained in the test beam: σ ~15.8ps/one MRPC detector [18].

This shows that MRPCs are potentially excellent TOF detectors, which are affordable for large-scale applications. The major problem is that the maximum rate capability is only ~1kHz/cm^2. This makes them presently unusable for applications at SuperB, Belle II or pp-diffractive scattering at LHC. However, there are some attempts to develop a low resistivity glass to improve their rate capability [18].

B. MCP-PMT detectors

Figure 7 shows the typical micro-channel plate PMTs (MCP-PMTs), which are commercially available. Table 4 summarizes their geometry, QE, type of photocathode, their single photoelectron transit time spread (σ_{TTS}), or simply TTS, and the risetime. To measure these parameters correctly, one needs a very fast oscilloscope[6], a very fast light source[7],

and the electronics must be as fast as the MCP-PMT[8]. As this is not always available, I quote mostly the upper TTS or risetime limit. Other variables will influence the timing resolution, for example, the S/N ratio or the cross-talk, which is a problem in multi-anode devices. All these factors make the TTS measurement at a level of 10-20ps rather hard and make the setup expensive.
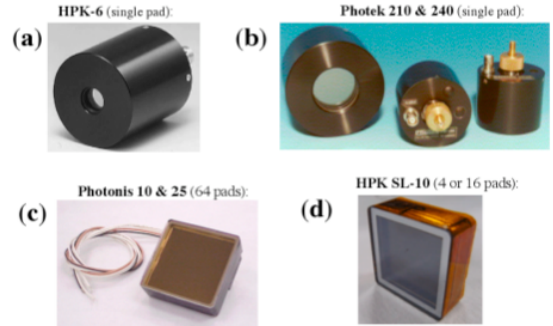
Fig. 7 MCP-PMTs used in recent beam tests: (a) Hamamatsu HPK-6 (also called R3809U-50-11X)., (b) Photek-210 & 240, (c) Photonis Planacon and (d) Hamamatsu SL-10. In this paper we consider only tubes with a double-MCP configuration.

Table 4: TTS & risetime of typical MCP-PMTs

MCP-PMT	# of anodes	MCP size	Hole [μm]	QE [%]	Photocathode	TTS [ps]	Risetime [ps]
HPK-6	1	φ11mm	6	26	Multi-alkali	~11 *	< 150 *
HPK-10	1	φ25mm	10	26	Multi-alkali	< 35 *	< 200
HPK SL-10	4	22x22	10	24	Multi-alkali	< 30 *, < 32 ᵉ	< 200 *
BINP-6	1	φ18mm	6	18	Multi-alkali	< 27 ᵉ	< 200
Photonis-10	64	49x49	10	24	Bi-alkali	< 30 ᵇ, < 32 ᶠ	< 400 ᶠ
Photonis-25	64	49x49	25	24	Bi-alkali	< 40 *, < 40 ᶠ, < 37 ᶜ	< 400 ᶠ
Photek-210	1	φ10mm	3.2	30	Multi-alkali	< 33 ᵈ, < 16 ᶠ, < 14 *	~81 *
Photek-240	1	40mm	10	30	Multi-alkali	< 40-45 ᵈ	~180 *

References: + [19], * [20], a [21], b [22], c[9] [23], d [24], e [25], f [29].
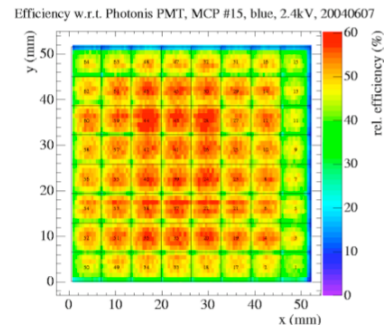
Fig. 8 Single photoelectron efficiency of the Photonis-25 normalized to the Photonis Quatacon PMT XP2262/B. It is less than 60% efficient, and this includes out of time hits in the tail of the distribution [26].

Although MCP-PMTs are very fast detectors, one must remember that there is a loss of photoelectrons at the entry to the MCP hole, thus reducing the S/N ratio. This is demonstrated in Fig.8, which shows a 2D single

---

[5] A 4-channel 10GSa/s digital oscilloscope was used instead of TDCs.
[6] 16-18GHz BW oscilloscope is needed to measure a risetime of < 200ps.
[7] For HPK-6 in Table 4, Hamamatsu [19] used C5594 1.5GHz BW amplifier and a Nd-YAG laser with FWHM ~5ps width, instead of typical laser diodes, providing a light width of FWHM ~30-35ps, which was used in most of the tests of Table 4.

[8] For Photek-210 in Table 4, A. Ronzhin [24] used 1GHz BW Ortec 9327CFD/566TAC/114ADC electronics; A. Brandt [29] used two Minicircuit ZX60 amplifiers (3 to 8 GHz BW, 10x) with a 2GHz filter to reduce the noise, Louvain CFD and 16 GHz BW, 80 GSa/s scope.
[9] A. Lehman has measured three Photonis-25 tubes, each giving a slightly different TTS value: XP85011 (49ps), XP85012 (37ps) and XP85013 (51ps) [23].

photoelectron efficiency scan of the Photonis-25 tube normalized to the Photonis Quatacon PMT XP2262/B [26], indicating that it is less than 50-60% as efficient, and this includes out-of-time hits in the tail of the distribution, i.e., the in-time efficiency is even lower by 20-30%. This loss has to be compensated by a longer radiator.

C. R&D test results with both MCP & radiator in the beam, and their possible applications

The Nagoya group [27] was the first to demonstrate that to achieve high-resolution timing with MCPs, one not only needs a fast detector coupled to a fast electronics, but one needs also a radiator producing Cherenkov light. They used the HPK-6 tube. This was followed by good test results in SLAC/Fermilab beam tests using Photonis Planacon-10 & 25 tubes [28] and Photek-240 tubes [24]. Table 5 shows the summary of all beam test results up to this point. In all cases both the MCP tube and the radiator were placed directly in the beam. The tests used two identical tubes to provide start/stop timing. The results in the table indicate resolutions per single tube.

Table 5: Beam test results obtained with the MCP-PMTs and the "radiator+window" located directly in the beam

MCP-PMT	# of anodes	Gain	Hole dia. [μm]	Window thickness [mm]	Radiator length [mm]	Npe	Resolution [ps]
HPK-6	1	$\sim 10^6$	6	3	10	~ 80	~ 6.2 [a]
Photonis-10	64	$\sim 2 \times 10^4$	10	2	10	~ 35	~ 14.0 [b]
Photonis-25	64	$\sim 10^6$	25	2	6	~ 30	~ 13.9 [b]
Photek-240	1	$\sim 10^6$	10	9.6	0	70-80	~ 7.7 [c]
Photek-210	1	$\sim 10^6$	3.2	5.6	0	45-50	~ 12 [c]
Photonis-25	64	$\sim 10^6$	25	2	0	~ 15	~ 37 [d]

References: a [27], b [28], c [24], d [31].

The Nagoya test [27] varied the radiator length[10] (L) during the beam test, while operating at high gain of $\sim 10^6$. The advantage of the high gain approach is that one can reduce the radiator thickness and still obtain a very good timing resolution. To illustrate this point, Fig.9a compares the Nagoya results and the author's calculation[11]. One can see that even a 3mm-thick window, used as a radiator, gives a very good result. On the other hand, the SLAC/Fermilab beam tests [28] with the Photonis-10 tube were run at low gain, motivated by rate and aging problems at SuperB factory due to a large single photoelectron background. The reason for this is that in e^+e^- machines most of the background is caused by gammas causing a few photoelectron deposits in the radiator. If one lowers the gain, one becomes sensitive to charged tracks only[12]. On the other hand, one has to have the radiator thick

enough to produce $N_{total} \sim 6\text{-}8 \times 10^5$ photoelectrons/track to get a sufficient S/N ratio for good timing. The radiator was made of Fused silica cubes with polished sides. The author's calculation is shown in Fig.9b. One can see that the main disadvantage of this approach is that the resolution degrades very rapidly as Npe (the number of photoelectrons) goes down for shorter radiator length. One can see that one needs at least 10 mm radiator length plus 2 mm window thickness to get good resolution at low gain.

(a)

(b)
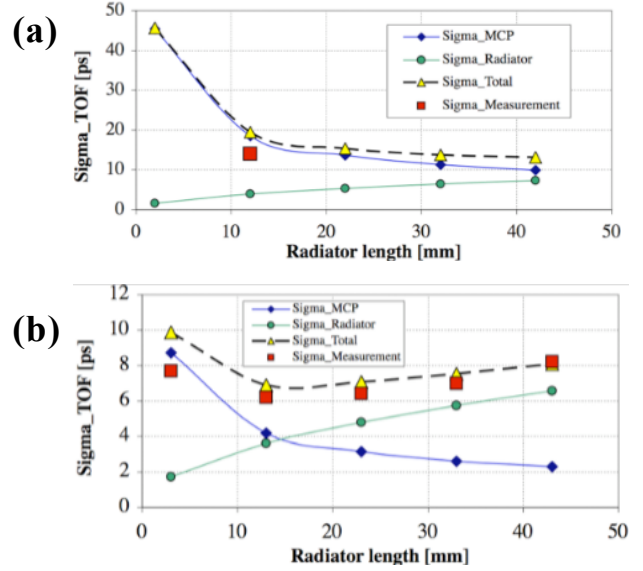
Fig. 9 (a) High gain operation:: Nagoya beam test results [27] compared to author's simple prediction, assuming $\sigma_{TTS}(Npe=1)\sim 32ps$. (b) Low gain operation: SLAC/Fermilab beam test results [28] with Photonis-10 MCP-PMT compared to author's simple prediction, assuming $\sigma_{TTS}(Npe$ extrapolated to $1)\sim 120ps$.

Table 5 also shows rather good results with a Photonis-25 tube, operated at high gain with a 6mm external radiator. It is equally good as the previous result with the Photonis-10 tube, operated at low gain. Table 5 also shows results with a Photonis-25 tube, operated at high gain, and a 2mm radiator made of a MCP window [31]. The result of $\sigma \sim 37ps$, obtained using a common "bottom MCP out" signal, was slightly worse than the above model's prediction, however, the common signal may be affected by a cross-talk more easily. Clearly, there is a trade-off between the high and low gain operation, perhaps, the low gain operation is not the best in terms of the highest possible resolution, however, it is better for aging and rate issues.
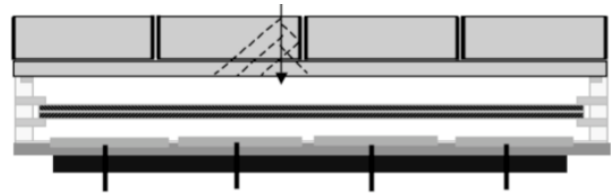
Fig. 10 A possible future pixilated TOF detector based on the Photonis Planacon MCP-PMT with pads arranged into 16 macro-pixels. The radiator consists of 16 cubes, each one optically isolated from other [32].

Figure 10 shows a possible application of the low gain operation concept proposed to SuperB for the endcap TOF

---

[10] They obtained ~ 20 photoelectrons (pe) for L = 3 mm, and 40-50 pe's for L = 10 + 3 mm. The best resolution was obtained for L = 10mm, with 3 mm window on MCP.

[11] (a) $\sigma_{TOF} \sim \sqrt{[\sigma^2_{MCP\text{-}PMT} + \sigma^2_{Radiator} + \sigma^2_{Pad\ broadenibng} + \sigma^2_{Electronics}]} = \sqrt{[(\sigma_{TTS}/\sqrt{N_{pe}})^2 + (((L*1000mm/cos_{qC})/(300mm/ps)/n_{group})/\sqrt{(12Npe)})^2 + ((5*1000mm/300mm/ps)/\sqrt{(12Npe)})^2 + (4.1\ ps)^2]}$; where σ_{TTS} (Npe =1)$\sim$ 32ps at high gain; example for L = 13 mm;
$$\sigma_{TOF} \sim \sqrt{[4.18^2 + 3.6^2 + 0.63^2 + 4.1^2]} \sim 6.9\ ps$$

[12] This approach may not wotk in proton machines where the background composition is different.

detector [32]. A similar concept is being considered for the Phoenix experiment TOF wall [33].

To progress significantly further with the TOF technique based on MCP-PMT detectors, it is important to bring their cost down; here an important contribution may come from the pioneering development of MCP designs within the LAPD collaboration [34].

D. Application in LHC pp-diffractive scattering, where the radiator is in the beam and the MCP is out of beam

Both ATLAS and CMS experiments at LHC plan to place several sets of TOF detectors close to the beam lines, measuring timing of diffractively scattered protons in an attempt to discover the Higgs particle. Even with the long flight distances to these counters, a timing resolution of ~10ps is required to reduce the background. High rate and aging problems prevent placing the MCPs directly into the proton flux. The solution is either (a) short multiple-bar quartz radiators in detectors called either Quartic [29] or Qbar [24] (Fig.11a), or (b) a C_4F_{10} gas radiator with a mirror in a detector called Gastof (Fig.11b). The quartz radiator contributes a considerable chromatic contribution and has to be kept short. Although a single bar contributes a resolution of only $\sigma \sim 40$ps, multiple bar measurements combined will deliver $\sigma \sim 10$ps. On the other hand, the C_4F_{10}-based radiator has very fast light production contributing $\sigma_{Radiator} < 1$ps, and thus this concept is limited by the detector only [30].
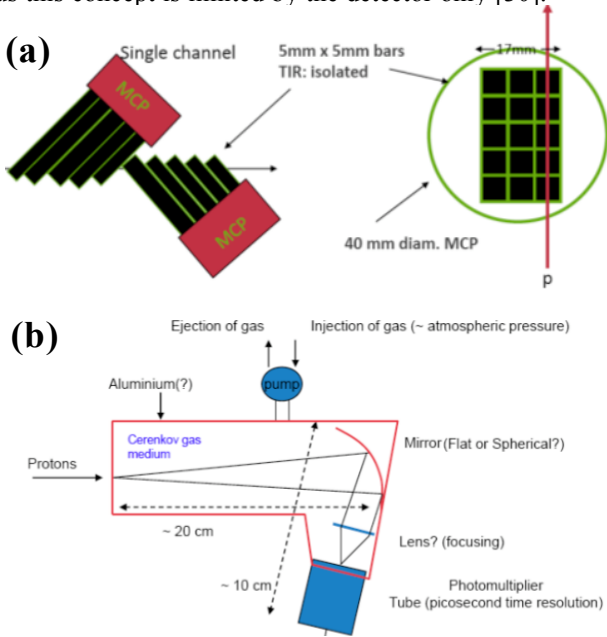
Fig. 11 (a) Principle of Qbar detector [24]. (b) Principle of Gastof detector. [30].

The first result from the Qbar detector beam tests at a Fermilab 120 GeV proton beam shows very good results. The two detectors used Photek-240 MCP-PMTs. With two detectors A&B mounted on the same side of the beam as it would be in LHC, so that the particle horizontal position cancels in the time difference, they measured $\sigma(A) = 15.5$ ps and $\sigma(B) = 16.3$ ps, so that the pair of counters (if considered as a single detector) had a resolution $\sigma(AB) = 11.2$ ps [24].

They plan to add more detectors in tandem to reduce the final error even further. However, to deal with very high multiplicities at the full LHC luminosity, one may have to use a segmented MCP-PMT such as what is planned for the Quartic detector [29].

These detectors have huge operational challenges at LHC due to very large background rates, close to the MCP maximum limit, and also due to the photocathode aging due to large charge doses.[13] Novel ideas will be required to make this possible, and a lot of testing. Possibly one has to replace them often.
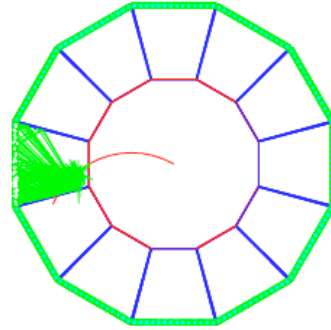
Fig. 12 The TOP-like TOF detector proposed for SuperB endcap [37]. The picture shows a MC simulation of a 900 MeV/c pion in one out of 12 sectors made of fused silica sheets. At the outer radius there are Hamamatsu SL-10 MCP-PMT detectors measuring an x-coordinate and a time of arrival of single photons.

E. DIRC-like TOF detectors

As shown in [35], the DIRC concept, employing internally reflecting photons in the quartz radiator, can derive its particle separation capability not only from its measurement of the Cherenkov angle, as in imaging RICH detectors such as the BaBar DIRC, but it can also separate particles as a TOF counter.[14] In this paper, we call these conceptually similar detectors DIRC-like TOF detectors [37,38]. They are also called TOP [21,36], and TORCH [39]. DIRC-like TOF detectors are devices where a quartz radiator is coupled to a string of fast MCP detectors measuring time and usually one space-coordinate only (the so-called x-dimension, which is approximately orthogonal to the typical average particle and photon propagation paths). The Cherenkov angle resolution is generally not sufficient to achieve good particle separation, when considered as a RICH detector [35]. However, the counter can be used as a high resolution TOF detector provided that the timing resolution is adequate, the individual photon path lengths can be determined with a modest number of ambiguities, and that the quartz piece is small enough to limit the chromatic broadening. Examples of such devices are (a) the short TOP counter initially proposed for Belle II [36], which clearly demonstrated a resolution of 40-50ps in the test beam, or (b) the recently proposed SuperB endcap TOF counter (see Fig.12) [37,38], which hopes to achieve a similar resolution.[15] The beauty of this concept is that the total

---

[13] A. Brandt quotes these numbers for a typical expected LHC operation: a current of $I_{max} \sim 3$ μA/cm^2, and a total charge doses of 35 C/cm^2/year [29].

[14] In fact the very first mention, to our knowledge, that DIRC can be used as a TOF can be found in B. Ratcliff, BaBar Note #92 (1992).

[15] $\sigma_{Total} \sim \sqrt{[\sigma^2_{Electronics} + (\sigma_{Chromatic}/\sqrt{(\epsilon_{Geometrical_loss} * N_{pe})})^2 + (\sigma_{TTS}/\sqrt{\epsilon * N_{pe}})^2 + \sigma^2_{Track} + \sigma^2_{detector\ coupling\ to\ bar} + \sigma^2_{to}]} \sim$30-40ps, where
$\sigma_{Electronics}$ - electronics contribution ~ 5-10 ps (WaveCatcher)
$\sigma_{Chromatic}$ - chromatic term = f (photon path length) ~ 10-25 (Geant 4)

number of photon detectors is small. On the other hand, these devices are more sensitive to background as they do not have the redundancy of the highly pixilated RICH detectors, which may also be readout in three dimensions. This is true especially in the region below the Kaon threshold, where a large background will fake Kaons into pions, and would make such device less useful (see more discussion on this topic in [40]). The threshold region is an important region for SuperB or Belle II physics.

F. TOF with G-APD

Geiger mode operating APD (Avalanche Photo-diode) detectors, also known under names such as G-APD, SiPMT (Silicon Photomultiplier), MPPC (Multi-Pixel Photon Counter), etc., have generated great interest recently in regards to possible TOF applications. Although specially prepared G-APDs achieved superb σ_{TTS} of 17ps [41], or 37ps [42], more typical values of commercial G-APDs are close to σ_{TTS} ~80-100ps. Nevertheless one can get a very good TOF timing resolution even with these devices if the radiator provides enough photoelectrons. Figure 13 shows a beam test result, performed recently at Fermilab in the 120GeV proton beam [24]. Coupling a single 3mm x 3mm Hamamatsu G-APD to a 3cm-long quartz radiator matching the G-APD's footprint of 3mmx3mm produced a timing resolution of σ ~16.3ps for a typical signal of ~60 photoelectrons. If one unfolds the contribution from a start counter (Photek-210 in this case), the G-APD resolution was σ_{G-APD} ~14.5ps. Although G-APDs are very sensitive to bias voltage and temperature (6.2ps/10mV & 11.5ps/0.5^{o}C [24]), it is possible to correct these effects by simply monitoring the pulse height.
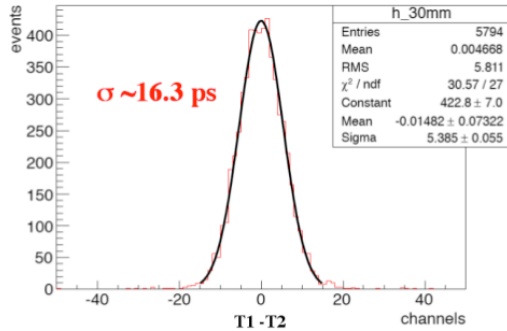
Fig. 13 The resolution obtained in the 120 GeV proton test beam at Fermilab with a single 3mm x 3mm G-APD coupled to a 3cm-long quartz radiator. The start signal was obtained from Photek-210 MCP-PMT .

G. TOF with a proximity focusing H-APD

A proximity focusing Hamamatsu H-APD (Hybrid-APD) is a combination of a vacuum tube with a uniform electric field and an avalanche photo diode (APD). These detectors are just emerging, and therefore not many parameters are known. They can operate in a large magnetic field, reach σ_{TTS} ~100ps [43], and obtain a gain of 10^4-10^5. With a quartz radiator they could be used very well for a good TOF detector application.

H. Electronics for TOF detectors

(a) MCP-PMT tests: The Nagoya beam test [27] used the commercial electronics Becker&Hickl SPC-134 CFD/TAC/ADC providing $\sigma_{Electronics}$ ~4.1ps and time scale calibration of 814fs/count. SLAC/Fermilab beam tests [28] used the commercial Ortec 9327CFD/566TAC/114ADC electronics providing $\sigma_{Electronics}$ ~3.4ps and time scale calibration of 3.17ps/count.[16] A. Brandt's group [29] used a tandem of two Mini-Circuit ZX60 amplifiers (10x each, 8GHz BW), followed by a 2GHz BW filter, a Louvain CFD [30] and 16 GHz BW, 40 GSa/s scope.

(b) The latest MRPC test beam used two LeCroy four-channel 10GSa/s oscilloscopes, believed to be contributing $\sigma_{Electronics}$ ~5ps [18].
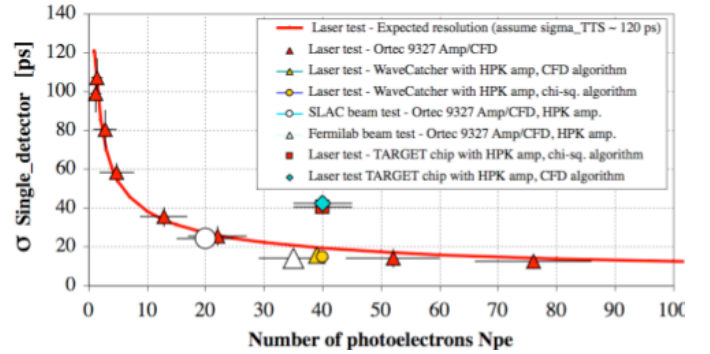
Fig. 14 The graph includes SLAC and Fermilab beam test results (large open circle and triangle) and laser tests, both using the Ortec CFD/TAC/ADC electronics, and waveform digitizers TARGET and WaveCatcher [46]. An important point is that the MCP-PMTs operated at low gain in all these tests.

(c) The question is if the new emerging waveform digitizing electronics [44,45] can start competing with the above mentioned commercial CFD electronics. The answer depends on the digitizer's front end BW, the S/N ratio and the sampling frequency. Recently, there was an attempt to start answering some of these questions empirically [46] using TARGET and WaveCatcher waveform sampling electronics, and a laser bench setup with two Hamamatsu C5594 1.5 GHz BW amplifiers with 63x gain. The paper [46] concluded that waveform digitizing timing results using the WaveCatcher board are consistent with SLAC/Fermilab beam test results, which used a combination of the Ortec 9327CFD, TAC588, and 14bit ADC114 electronics – see Fig.14. The TARGET chip results are worse due to (a) lower bandwidth, (b) worse S/N ratio, and (c) lower sampling frequency.[17] Similar conclusions about the exquisite timing possible with waveform digitizing techniques was shown in [47], where the authors compared simulations with measurements using an 18GHz BW oscilloscope operating at 40GSa/s sampling.

σ_{TTS} - transit time spread ~ 35-40 ps

σ_{Track} - timing error due to track length L_{path}: ~ 5-20 ps (Fast Sim)

$\sigma_{detector\ coupling\ to\ bar}$ - coupling to the bar ~ 1-20 ps (Fast Sim)

σ_{to} - start time dominated by the SuperB crossing bunch length ~ 15-20 ps

[16] Measured by the author using a special time calibration pulser made by Impeccable Instruments. A. Ronzhin of Fermilab measured $\sigma_{Electronics}$ ~2ps with the same electronics, but calibrated it using the micrometer-based delay line.
[17] TARGET: 150MHz BW, S/N ~40-50, sampling rate of 450ps/bin,
   WaveCatcher: 500MHz BW, S/N ~450, sampling rate of 312ps/bin.

CONCLUSION

The TRD technique is mature and has been tried in many hadron colliders. It needs space though, about 20cm of detector radial space for every factor of 10 in the π/e rejection power, and this tends to make such detectors large.

Although the cluster counting technique is an old idea, it was never tried in a real physics experiment. Recently, there are efforts to revive it for the SuperB experiment using He-based gases and waveform digitizing electronics. A factor of almost 2 improvement, compared to the classical dE/dx performance, is possible in principle. However, the complexity of the data analysis will be substantial.

The TOF technique is well established, but introduction of new fast MCP-PMT and G-APD detectors creates new possibilities. It seems that resolutions below 20-30ps may be possible at some point in the future with relatively small systems, and perhaps this could be pushed down to 10-15ps with very small systems, assuming that one can solve many systematic issues. However, the cost, rate limitation, aging and cross-talk in multi-anode devices at high BW are problems. There are several groups working on these issues, so progress is likely.

Table 6 summarizes the author's opinion of pros and cons of various detectors presented in this paper based on their operational capabilities. We refer the reader to Ref.40 for discussion of other more general limits from the PID point of view.

Table 6: Major pros and cons of various detector schemes

Detector	PRO	CON
MRPC	- TOF detector timing resolution limit with a 24gaps/MRPC : ~10 ps. - Can be built in very large sizes. - Very cheap technology.	- Charged particle rate limited to ~1kHz/cm^2 presently - 24 gaps/MRPC represents ~14% of X_o without the electronics
MCP-PMT	- TOF detector resolution limit: ≤ 5 ps. - σ_{TTS}: ~ 10-30 ps - Probably the fastest detector available. - "Bottom MCP electrode" is very useful.	- Very expensive technology presently. This limits this technology to small TOF detector systems at present. - Relative single photoelectron efficiency response compared to Photonis Quantacon XP 2272B PMT is typically less than 50-60% at 407nm.. "In time" response is even 20-30% lower due to tail. This reduces the S/N ratio. - Cross-talk between anodes for high BW amplifiers - Photonis Planacon MCP-PMT represents ~14% of X_o
G-APD	- σ_{TTS}: ~17-100 ps - TOF timing resolution limit: ≤ 15ps - No sensitivity to magnetic field - Relative cheap technology	- Sensitive to neutron background for a total integrated flux of >10^{10} neutrons/cm^2 - Very sensitive to bias voltage and temperature
H-APD	- σ_{TTS}: ≤ 100 ps - No sensitivity to magnetic field	- Not yet available - Total gain is only 10^4-10^5.
Drift chamber with cluster counting	- Improvement in PID performance up to a factor of 2 compared to a classical dE/dx	- Requires sampling rate of ~1.5 GSa/s, ~500MHz amplifier BW, 8 bit ADC dynamical range - Data analysis of waveforms could be very complex - The He/iC$_4$H$_{10}$ gas mix has to be tuned very carefully.

REFERENCES

[1] ATLAS Collaboration, ATLAS Inner Detector Technical Design Report, Volume 2,CERN/LHCC/97-16, 30 April 1997.
[2] A.H. Walenta, IEEE Trans.Nucl.Sci., NS-26(1979)73.
[3] F. Lapique and F. Piuz, Nucl.Instr.& Meth., 175(1980)297.
[4] V. Eckart et al., Nucl.Instr.& Meth., 143 (1977)235.
[5] P. Rehak and A.H. Walenta, IEEE Trans.Nucl.Sci., NS-27(1980)54.
[6] A. Breskin anf R. Chechik, Nucl.Instr.& Meth., A252 (1986)488.
[7] A. Pansky, WIS-92/5/Mar-PH.
[8] G. Malamud, A. Breskin and R. Chechik, WIS-95/38/Aug.-PH.
[9] G.Cataldi,F.Grancagnolo,S.Spagnolo, Nucl.Instr.& Meth A386(1997)458.
[10] J. Va'vra, Nucl.Instr.& Meth A453(2000)262-272.

[11] Akimov et al. Nucl. Instr. & Meth., 344 (1994) 120-124.
[12] A.Arefiev et al. Nucl. Instr. and Meth., 348 (1994) 318-323.
[13] Y.N.Pestov. Proc. 4th San Miniato Topical Seminar, World Scientific, 1991 p. 156.
[14] C. Williams, "TOF with MRPC", Proceedings of Erice workshop, 2003.
[15] Katayoun Doroud, "ALICE TOF system", Ph.D. thesis, CERN, 2010.
[16] STAR MRPCs, Nucl. Instrum. Meth. A 558 (2006) 419.
[17] CBM MRPCs, http://cbm-wiki.gsi.de/cgi-bin/view/Public/PublicTof.
[18] C. Williams, private communication, CERN, 2010.
[19] Hamamatsu Co. data sheets for MCP-PMT R3809U-50, which is HPK 6 tube label used in this paper..
[20] J. Howorth, Photek, "ps-workshop", 2008, Lyon, France.
[21] K. Inami, RICH 2010 workshop, Cassis, France, 2010.
[22] J. Va'vra et al., "A 30 ps timing resolution for single photons with multi-pixel Burle MCP-P", Nucl. Instr.& Meth., A 572 (2007) 459–462.
[23] A. Lehman, RICH 2010 workshop, Cassis, France, 2010.
[24] A. Ronzhin, M. G. Albrow, M. Demarteau, S. Los, S. Malik, A. Pronko, E. Ramberg, A. Zatserklyaniy, "Development of a 10 Picosecond Level Time of Flight System in the Fermilab Test Beam Facility," submitted to Nusl.Instr.&Meth.
[25] S. Korpar et al, Nucl.Instrum.Meth.A595(2008)169-172.
[26] C. Field, T. Hadig, D.W.G.S. Leith, G. Mazaheri, B. Ratcliff, J. Schwiening, J. Uher, and J. Va'vra, Nucl.Instr.& Meth., A553(2005)96-106.
[27] K. Inami, H. Kishimoto, Y. Enari, M. Nagamine, and T. Ohshima, "A 5 ps TOF-counter with MCP-PMT", Nucl. Instr. & Meth., A560(2006)303-308.
[28] J. Va'vra, D.W.G.S.Leith, B.Ratcliff, E.Ramberg, M.Albrow, A.Ronzhin, C.Ertley, T.Natoli, E. May, K. Byrum, Nucl. Instr.& Meth. A606(2009)404-410.
[29] A. Brandt, Quartic detector, private communication, and a talk at the "ps timing workshop", Clermont-Ferrand, January 28, 2010.
[30] K. Piotrzkowski, Gastof detector, RICH 2010 workshop, Cassis, France, 2010, to be published in Nucl.Instr.& Meth.
[31] S. Korpar et al., Nucl..Instr.&Meth.A595(2009)169-172.
[32] J. Va'vra, "Pixilated TOF detector for SuperB endcap", SuperB workshop, http://agenda.infn.it/conferenceDisplay.py?confId=1161, Perugia, Italy, 2009.
[33] C. Woody, private communication.
[34] H. Frisch et al., R&D effort to develop new MCP structures by the University of Chicago, Argonne Natl. lab, and the Space Scienec lab, Berkely, CA., and O. Siegmund, LAPPD collaboration: "Large Area Picosecond Photodetectors", RICH 2010 workshop, Cassis, France, 2010, and M. Wetsten, LAPPD collaboration: "Big, fast and cheap", RICH 2010 workshop, Cassis, France, 2010.
[35] B.Ratcliff, contribution to the ICFA Inst. Bulletin, 2001 http://www.slac.stanford.edu/pubs/icfa/spring01/paper2/paper2a.html
[36] K.Inami, "ps-workshop", 2008, Lyon, France.
[37] J. Va'vra, "Forward TOF", SuperB workshop, Orsay, France, Feb. 2009, http://agenda.infn.it/conferenceDisplay.py?confId=959.
[38] L. Burmistrov, N. Arnaud, O. Bezshyyko, H. Dolinskaya, A.Perez, A. Stocchi, "Geant4 simulation of the DIRC-like forward TOF detector", SuperB workshop, Frascatti, Dec. 2009, http://agenda.infn.it/conferenceDisplay.py?confId=1165
[39] M. Charles and R. Forty, TORCH, RICH 2010 workshop, Cassis, France, 2010.
[40] B. Ratcliff, Nucl..Instr.& Meth., A595(2008)1-7.
[41] G-APD "id-100" made by Quantique Co., Switzerland, their measurements.
[42] Measurement by J.Va'vra with PiLas laser at 635nm, results mentioned in Ref.26. (G-APD designed by Sopko, active quenching circuit by Prochazka, CVUT Prague).
[43] I. Adachi, R. Dolenec, K. Hara, T. Iijima, H. Ikeda,Y. Ishii, H. Kawai, S. Korpar, Y. Kozakai, P. Krizan, T.Kumita, E. Kuroda, Y. Miyazawa, S. Nishida,I. Nishizawa, S. Ogawa, R. Pestotnik, N.Sawafuji, S. Shiizuka, T. Sumiyoshi, M. Tabata, Y.Ueki, and Hamamastu Co., RICH 2010 workshop, Cassis, France, 2010.
[44] G. S. Varner, L. L. Ruckman and H. Tajima, "Design and Performance of the TeV Array with GSa/s sampling and Experimental Trigger (TARGET)ASIC", To be published in Nucl.Instr.& Meth., and G.S. Varner, L.L. Ruckman, J.W. Nam, R.J. Nichol, J. Cao, P.W. Gorham, M. Wilcox, "The large analog bandwidth recorder and

digitizer with ordered readout (LABRADOR) ASIC," Nucl. Inst.& Meth. A 583 (2007) 447.

[45] E. Delagnes, Y. Degerli, P. Goret , P. Nayman, F. Toussenel, P. Vincent, "SAM: A new GHz sampling ASIC for the HESS-II front-end electronics," Nucl..Instr. & Meth. A567:21-26, 2006.

[46] D. Breton, E. Delagnes, J. Maalmi, K. Nishimura, L.L. Ruckman, G. Varner, and J. Va'vra, "High resolution photon timing with MCP-PMTs: a comparison of commercial constant fraction discriminator (CFD) with ASIC-based waveform digitizers TARGET and WaveCatcher.", SLAC-PUB-14048, June 16, 2010, to be published in Nucl..Instr.& Meth.

[47] J.-F. Genat, G. Varner, (Hawaii U.) , F. Tang, H. J. Frisch, Nucl.Instr.& Meth., A607:387-393,2009